Theoretical elastic tensile behavior of muscle fiber bundles in traumatic loading events

Atsutaka Tamura [a, b, *], Jun-ichi Hongu [b], and Takeo Matsumoto [a,c]

[a] Nagoya Institute of Technology, Gokiso-cho, Showa-ku, Nagoya, Aichi 466-8555, Japan

[b] Tottori University, Koyama-minami, Tottori, Tottori 680-8552, Japan (Present affiliation)

[c] Nagoya University, Furo-cho, Chikusa-ku, Nagoya, Aichi 464-8603, Japan (Present affiliation)

* Corresponding author: a-tamura@tottori-u.ac.jp

Word count: 248 for abstract and 4668 for main text excluding references and legends.

ABSTRACT

Background: The mechanical characterization of skeletal muscle under high-rate loading regimes is important for predicting traumatic injuries due to traffic accidents and contact sports. However, it is difficult to perform dynamic mechanical tests at rates relevant to such rapid loading events.

Methods: In the present study, a series of stress relaxation tests were conducted on rabbit hind-limb muscle fiber bundles using a custom tensile tester. Using relatively moderate loading conditions compared to those typically associated with traumatic injuries, the passive stress-decaying mechanical properties of muscle fiber bundles were characterized. In addition, stress relaxation responses to various ramp-hold stretches were theoretically predicted by a custom-built code.

Findings: The results showed that the muscle fiber bundles exhibit greater stress relaxation at higher loading rates and greater stretch magnitudes. Based on these results, the data points representing the "elastic" stress–strain tensile behavior typical of traumatic injury were extrapolated using curve fitting. The theoretical model revealed rate-dependent characteristics of the muscle fiber bundles under traumatic loading conditions, which would result in tensile strengths of 300–500 kPa at the maximum engineering strain of 54%. This strength is on the order of magnitude as the maximum isometric stress of an active muscle contraction.

Interpretation: The proposed numerical model is expected to serve as a powerful research tool to investigate injury mechanisms of the skeletal muscle. Moreover, the elastic response that was theoretically predicted here will be useful in the development of effective countermeasures to prevent traumatic injuries due to rapid loading events.

Keywords: stress relaxation, muscle fiber bundle, uniaxial stretch, viscoelasticity, elastic response, traumatic injury

1. Introduction

Viscoelastic soft tissue exhibits stress relaxation in response to externally applied displacements such as extension, compression, or shear deformation. When a step-like displacement is given instantaneously and the displacement is held constant, soft tissue initially behaves like a nonlinear spring by instantly exerting a reaction force that decays over the course of holding period (the duration in which the displacement is held constant). For skeletal muscle, this phenomenon has a damping effect on the quickly applied deformation, thereby stabilizing the musculoskeletal system. On the other hand, skeletal muscle works actively as an actuator in the human body, contracting at a rate of 1–2 s^{-1} during daily activity (Lieber, 1997) and reaching maximum rates ranging between 5–10 s^{-1} (Lai et al., 2018). Since most muscles in the body work in antagonistic pairs, it is important to investigate the mechanical properties of muscle during both passive tension and active contraction. For instance, when the biarticular muscle group contracts voluntarily or compulsively, not only agonist but also antagonist muscles are typically recruited and the rate of passive stretching is equivalent to that of active muscle contraction.

Many nonlinear viscoelastic models have been formulated to characterize the complex passive mechanical properties of soft tissues. Of these models, the quasi-linear viscoelastic (QLV) theory, which was originally developed by Fung (1967, 1993), is the most widely accepted model for representing the viscoelasticity of soft biological materials. According to the QLV theory, the stress relaxation behavior can be expressed as a product of the separable functions of time, t, and strain, ε, as given by Eq. 1:

$$\sigma(t, \varepsilon) = G(t)\, \sigma^{e}(\varepsilon) \qquad \text{(Eq. 1)}$$

where $\sigma^{e}(\varepsilon)$ represents the instantaneous stress, which is defined as the elastic response to an idealized step-like strain, ε, at $t = 0$ (true zero). $G(t)$ is the reduced relaxation modulus representing the time-dependent stress response normalized to the measurable peak stress, σ_{0+} at $t = 0+$, which is defined for a ramp displacement completed with a rise time ($t_R = 0+$ was set to be as 0.4, 0.5, 1, or 6 s in the current work), as shown in Eq. 2; the QLV theory commonly assumes that the reduced relaxation modulus is independent of the applied strain.

$$G(t) = \sigma(t, \varepsilon) / \sigma_{0+} \qquad \text{(Eq. 2)}$$

However, a major limitation of the QLV model is that the initial portion of the stress relaxation cannot be measured experimentally because it is impossible to ramp the strain at an infinite rate (i.e., apply a true step-like strain). Thus, the "elastic" response measured with a high-rate loading regime inevitably includes the effect of stress relaxation during the ramp-phase period (i.e., the rise time, t_R). In such cases, a method of back-extrapolation is useful to modify the reduced relaxation modulus (Myers et al., 1991; Funk et al., 2000; Tamura et al., 2002). Nevertheless, it is impossible to perfectly compensate for the material behavior during the rise time (i.e., the initial stress relaxation).

In soft biological materials, it is known that the magnitude of the instantaneous stress increases as the applied displacement is increased and decreases as the rise time is extended. It should be noted that a common injury in athletes is muscle strain, which often occurs in the weakened or injured muscle following a "ballistic" high-force eccentric contraction (LaStayo et al., 2003). Thus, it can be expected that the impact velocity affects the pattern and severity of a traumatic injury to the musculoskeletal system (e.g., muscle tears and contusions). Therefore, it is crucial to characterize the behavior of tissue at high strain rates in order to accurately represent the muscle mechanics in computational models. In our previous study (Tamura et al., 2016), we examined the rate sensitivity of muscle fiber bundles subjected to uniaxial stretching in the velocity range of 0.02–0.5 s^{-1}. However, the passive mechanical properties of muscle fiber bundles in considerably high-rate loading conditions could not be examined due to the mechanical restriction of the custom tensile tester that was used (i.e., the applicable maximum velocity was limited to 20 mm/s). Since the rate sensitivity of soft tissue materials arises from the effects of stress relaxation, it is critically important to investigate its mechanical response to a step-like displacement (i.e., displacement with a "minimal" rise time). Hence, in the present study, we conducted a series of stress relaxation tests with a sub-traumatic but repeatable loading condition using freshly isolated muscle fiber bundles procured from the hind limbs of rabbits. Then, the obtained data were applied to theoretically predict the dynamic tensile behavior and elastic response of muscle fiber bundles that can be expected with a traumatic impact injury or ballistic loading conditions.

2. Methods

2.1 *Mechanical testing*

The specimen preparation, construction of the custom tensile tester, and data analysis were conducted as described elsewhere (Tamura et al., 2016). In brief, four male Japanese white rabbits weighing 2.6 ± 0.1 kg (mean ± SD) were used. The handling of all study animals was performed with

the approval of the Committee of Animal Experimentation of Nagoya Institute of Technology. The hamstrings were dissected from the hind limbs of the rabbits at room temperature immediately after sacrifice. The samples were tied to glass rods to retain their natural lengths and stored in a 50% (v/v) glycerol relaxing solution overnight (16–18 h), at 4°C. Then, single muscle fiber bundles of 30–40 mm in length and approximately 1 mm in diameter were carefully separated from the tissue using fine forceps and a dissection needle.

Each isolated specimen was mounted on the tensile tester with a pair of custom parallel-plate load cells (channels 1 and 2). Both ends of the specimen were glued to the tips of the cantilever arms using a cyanoacrylate adhesive. The initial distance between the innermost points of the grips on the two arms was adjusted to 20 mm (Fig. 1). The force data from each channel was recorded at a frequency of 1 kHz (NR-ST04, Keyence, Osaka, Japan); zero strain was defined as the first point at which the sum of the forces collected in the two channels constantly exceeded 0.1 mN. An image of the fiber bundle was captured by a digital camera (EX-ZR400, Casio, Tokyo, Japan) from both the top and side views using a mirror inclined a 45° angle to measure length, width, and height of the undeformed specimen. In addition, video was recorded during each test at 30 fps and consecutive still images were extracted for *post-hoc* image analysis.

After the experiment, ImageJ version 1.50 (National Institutes of Health, Bethesda, MD, USA) was used to perform dimensional measurements of each sample. In this study, we assumed that the cross-section of a fiber bundle specimen had an oval shape and measured the length of its major and minor axes. Consequently, the cross-section area of the specimen was 0.657 ± 0.022 mm^2 on average (mean ± SEM, n = 50), and the force data were converted to nominal stresses. The axial stretch along the fiber bundle was calculated ~~as the engineering strain~~ by dividing the current elongation by the initial grip-to-grip length of the specimen.

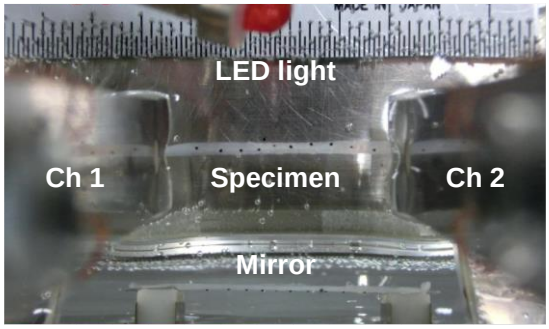

(a) Undeformed configuration at zero strain.

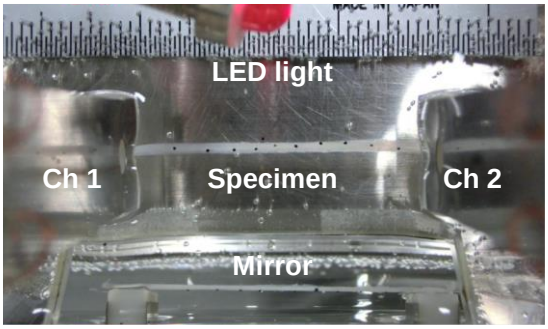

(b) Deformed configuration at maximum stretch.

Fig. 1: Typical deformation of a muscle fiber bundle during stress relaxation test with a 6 mm stretch (Top view); black dots placed upon the specimen along axial direction were vanilla beans. Ch 1 and Ch 2 indicate the left and right arm-tips of a pair of custom force transducers, respectively.

2.2 *Stress relaxation test*

The loading path included five cycles of preconditioning, a 120 s resting period, a rapid stretch up to a final displacement of 2, 4, 6, or 8 mm, each of which was followed by a 300 s holding period. During this period, the applied displacement was held constant throughout. In the preconditioning cycles, a uniaxial stretch was applied to fiber bundle at the rate of 2 mm/s until the specimen reached approximately 30% strain (6 mm displacement). The residual slack recovered completely during the resting period. The final stretch was applied at 5, 10, 15, and 20 mm/s (0.25, 0.5, 0.75, and 1 s^{-1}) for final displacements of 2, 4, 6, and 8 mm, thus maintaining a rise time, t_R, of 400 ms. The holding period of 300 s was considered to provide enough data points to identify the trend associated with the stress relaxation effects. In our previous work (Tamura et al, 2016), a muscle fiber bundle subjected to uniaxial stretch mechanically failed when a 12–16 mm displacement was applied. In the current work, therefore, the maximum displacement, 8 mm, was chosen as a range where a plastic deformation or any damage of the fiber bundle did not occur. The temperature of the specimen bath was maintained at 37°C by a hot plate (FHP-30S, TGK, Tokyo, Japan). All the experiments were completed within 30 h of harvesting.

2.3 *Statistical analysis*

Analysis of variance (ANOVA) was conducted for investigating the change in stress relaxation rates using SPSS version 24 (IBM, Armonk, NY, USA). *P*-values of 0.05 or less were considered to be statistically significant.

2.4 *Viscoelastic formulation*

Ideally, the parameters representing the stress relaxation should be uniquely identified by a fitting procedure with a step-like strain. Nevertheless, since it is physically impossible to apply a true step input, previous studies have employed a high-rate ramp as a close alternative to a step-like displacement (Tamura et al., 2007, 2008). With this approach, however, artifacts and measurement errors associated with the high strain rates (e.g., overshoot and vibration) might be introduced into the estimation of the parameters. Therefore, in the present study, the predictions were made based on the stress relaxation

responses to various ramp-hold stretches avoiding such unwanted contaminants or biases. This was done by collecting a series of relaxation curves under moderate loading conditions and approximating the elastic response using a least-squares method (Fig. 2).

Troyer et al. (2012) previously proposed a systematic method to correct for a finite-ramp time in an experiment to characterize the stress relaxation of the spinal cord. Based on this approach, our group has demonstrated that the uniaxial nonlinear viscoelastic behavior of a spinal nerve root can be represented in a simplified manner as follows (Tamura et al., 2017):

$$\sigma[\varepsilon(t), t] = \int_0^t E[\varepsilon(\tau), t-\tau] \frac{d\varepsilon(\tau)}{d\tau} d\tau + \sigma_0 \qquad \text{(Eq. 3)}$$

where σ is the stress, ε is the strain, t is the time, τ is the time variable of integration, and $E(\varepsilon, t)$ is the material relaxation modulus that represents the time-dependent relationship between stress and strain. The relaxation modulus of a material can be approximated by Eq. 4 as a Prony series:

$$E(\varepsilon, t) = \sum_{\mathrm{i}=1}^{5} E_{\mathrm{i}}(\varepsilon) e^{-t/\tau_{\mathrm{i}}} \qquad \text{(Eq. 4)}$$

where $E_{\mathrm{i}}(\varepsilon)$ is a strain-dependent variable corresponding to the time constant, τ_{i} (i = 1–5). In the present study, decadal time constants (τ_1 = 0.1, τ_2 = 1, τ_3 = 10, τ_4 = 100, and τ_5 = 1000 s) were selected to capture both the short-term and long-term material behaviors. Thus, the material stiffness can be described by the parameters E_{i} (i = 1–5) while the stress relaxation process can be described by the time constants τ_{i} (i = 1–5). With respect to the relaxation function, Quapp and Weiss (1998) have shown that a combination of exponentials is suitable as the original continuous function and allows efficient computational implementation. Preliminary testing revealed that five exponential terms were sufficient to fit the experimental data to Eq. 4. Since the equilibrium state stress at infinite time was not experimentally obtained, the stress relaxation was continued over 100 s to ensure that it is sufficiently long to study the relevant effects of ballistic behavior. For each test condition, the averaged stress relaxation data were fitted using a custom code in MATLAB R2017b, (MathWorks, Natick, MA, USA). Then, a nonlinear least-squares algorithm was used to identify the values of E_{i} (i = 1–5) yielding a stress response that is consistent with those obtained experimentally; specifically, the stiffness coefficients were obtained by minimizing the sum of the squared errors between the observed stress and the predicted stress during the ramp-hold stretch.

For further simplification, the passive elements of the muscle fiber bundle were assumed to work as linear springs during the ramp phase so that the reaction force would increase linearly in response to the applied displacement. Hence, the stress at any time point can be expressed in the form of an integral as shown in Eq. 5.

$$\sigma[\varepsilon(t),t] = E[\varepsilon(t),t-t]\varepsilon(t) - E[\varepsilon(0),t-0]\varepsilon(0) - \int_0^t \frac{dE[\varepsilon(\tau),t-\tau]}{d\tau}\varepsilon(\tau)d\tau + \sigma_0 \qquad \text{(Eq. 5)}$$

The fitting procedure proposed herein was validated using two sets of load-relaxation curves: 1) data from preliminary stress relaxation experiments with a constant 6 mm stretch with different rise times, t_R = 0.5, 1, 6 s (N = 1 for each condition), and 2) data from an additional series of stress relaxation experiments or main study with different ramp loadings up to 2–8 mm stretch with a constant rise time of t_R = 0.4 s (N = 3 for each condition). Thus, the theoretical elastic response to each stretch level was calculated by substituting t = 0 into Eq. 6 as shown in Fig. 2.

$$\sigma[\varepsilon(t),t] = E[\varepsilon(t),0]\varepsilon(t) - \int_0^t \frac{dE[\varepsilon(\tau),t-\tau]}{d\tau}\varepsilon(\tau)d\tau \qquad \text{(Eq. 6)}$$

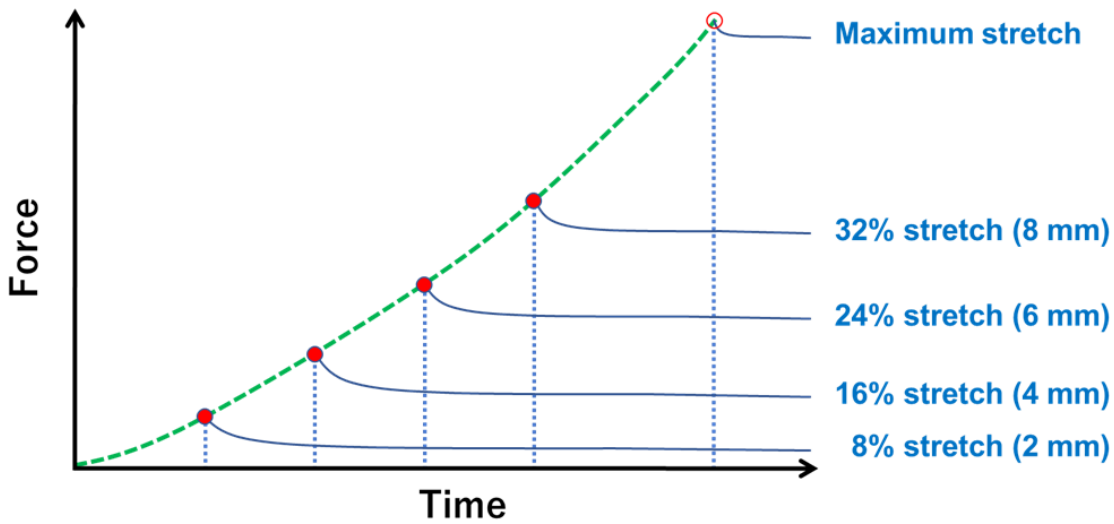

Fig. 2: Curve fitted to the instantaneous elastic response data based on a series of stress relaxation responses; the maximum stretch was assumed to be 54% engineering strain as determined in our previous study (Tamura et al., 2016).

3. Results

3.1 *Effect of the rise time on the stress relaxation response*

As a preliminary study, a series of stress relaxation tests were conducted with a constant maximum displacement of 6 mm ($N = 1$; number of rabbit). During the test, the muscle fiber bundles were subjected to ramp-hold stretches of rise times, $t_R = 0.5$, 1, and 6 s, which corresponded to rates of 12, 6, and 1 mm/s, respectively. As shown in Fig. 3a, the reduced relaxation modulus (i.e., the normalized mean stress relaxation response) did not change significantly following the ramp period until approximately 0.02 s after the maximum strain and ultimately reached an equilibrium state at 300 s that was consistent regardless of t_R. However, the stress relaxation behavior of muscle fiber bundles depended on the assigned rise time (i.e., the given loading rate): when the stretch was applied more rapidly, the stress decayed more swiftly after the ramp period.

3.2 *Effect of the maximum stretch on the stress relaxation response*

Another series of stress relaxation tests were performed at a constant rise time, $t_R = 0.4$ s ($N = 3$). Each of the normalized mean stress responses decayed over the period of 300 s as observed in the preliminary study (Fig. 3b). Nevertheless, the peak stress at the rise time, σ_{0+} (i.e., the instantaneous maximum stress immediately after the ramp period), and equilibrium state stress, σ_{100} (i.e., the stress measured after 100 s), increased significantly as the rate and the magnitude of the applied displacement were increased (Fig. 4). This is consistent with the results reported by Meyer et al. (2011) and Wheatley et al. (2016), which independently revealed that the stress relaxation response of skeletal muscle depends on the strain at the single fiber and tissue levels, respectively. In addition, to examine changes in material viscous behavior, a stress relaxation rate was determined, i.e., linear stress relaxation rates were computed based on the change in post-peak stress for four time periods of 0+ (t_R) –0.1, 0.1–1, 1–10, and 10–100 s. It was found that the stress relaxation rate also significantly depended on the magnitude of the applied stretch (the differences were statistically significant as shown in Fig. 5). Notably, some degree of stress relaxation would be expected, even during the initial ramp period. The stress relaxation rate during the measurable zero ($t_R = 0+$) and 0.1 s was much greater than that during other time periods (0.1–1, 1–10, and 10–100 s), indicating that significant energy dissipation occurred during the ramp period.

Based on these results, we hypothesized that the instantaneous stress and maximum reaction force of a muscle fiber bundle in response to a ramp stretch explicitly depends on both the applied loading rate and the peak displacement.

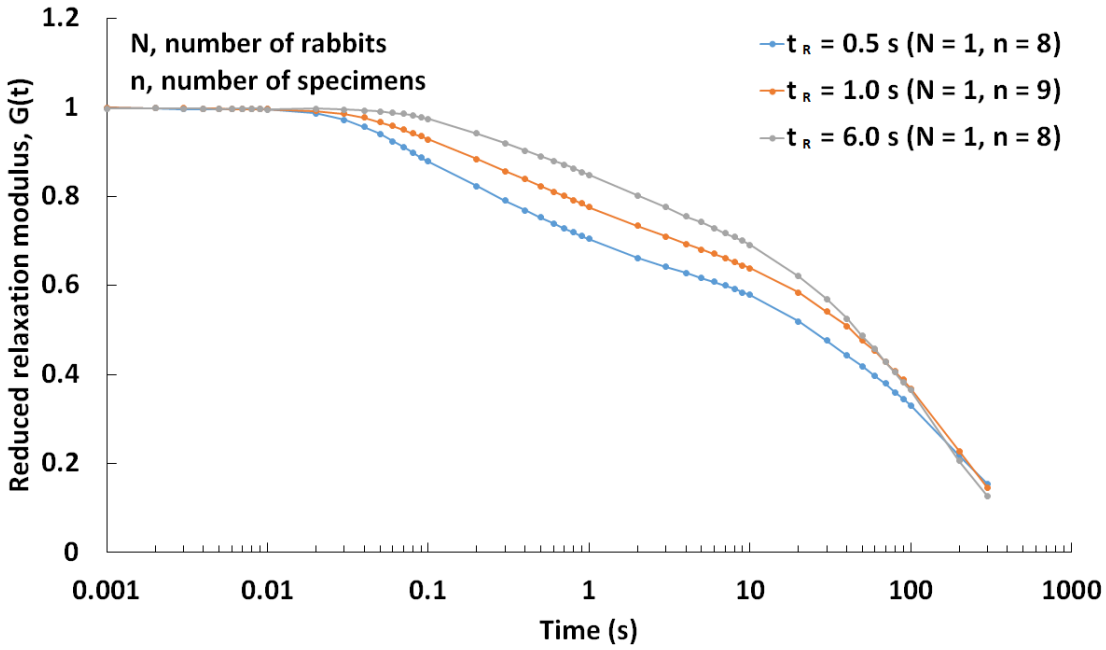

(a) Preliminary study: maximum stretch of 6 mm with rise times of t_R = 0.5, 1, and 6 s (N = 1).

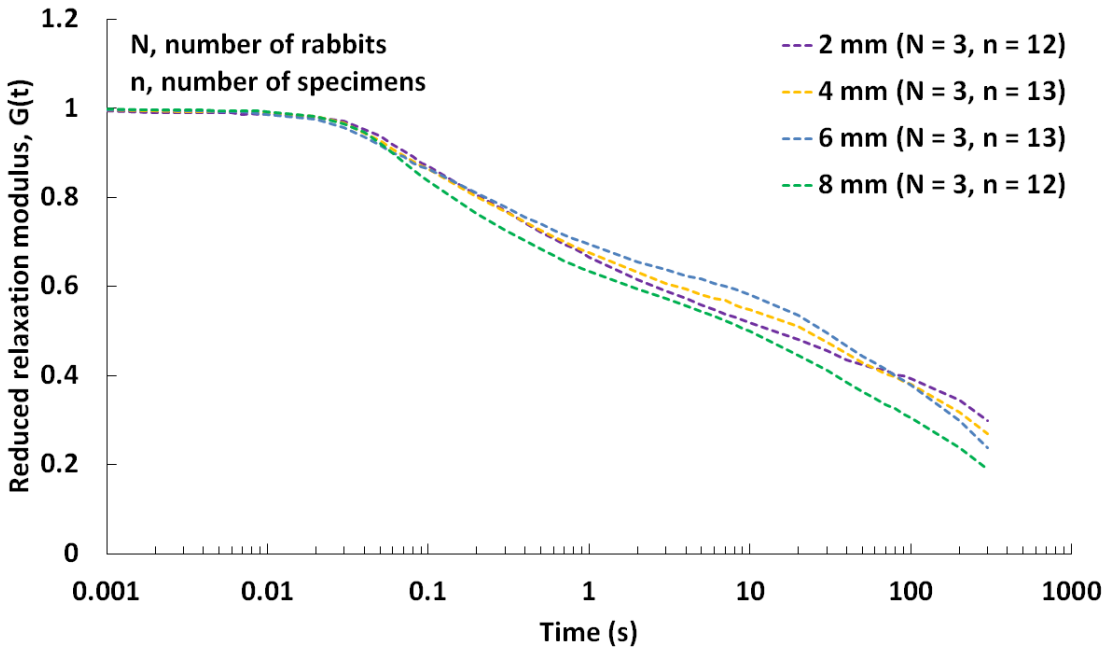

(b) Main study: maximum stretch of 2–8 mm with a constant rise time of t_R = 0.4 s (averaged for N = 3).

Fig. 3: Normalized mean stress relaxation responses with various maximum stretches and rise times (N, number of rabbits), implicating that material relaxation should be described as a function of time and stretch.

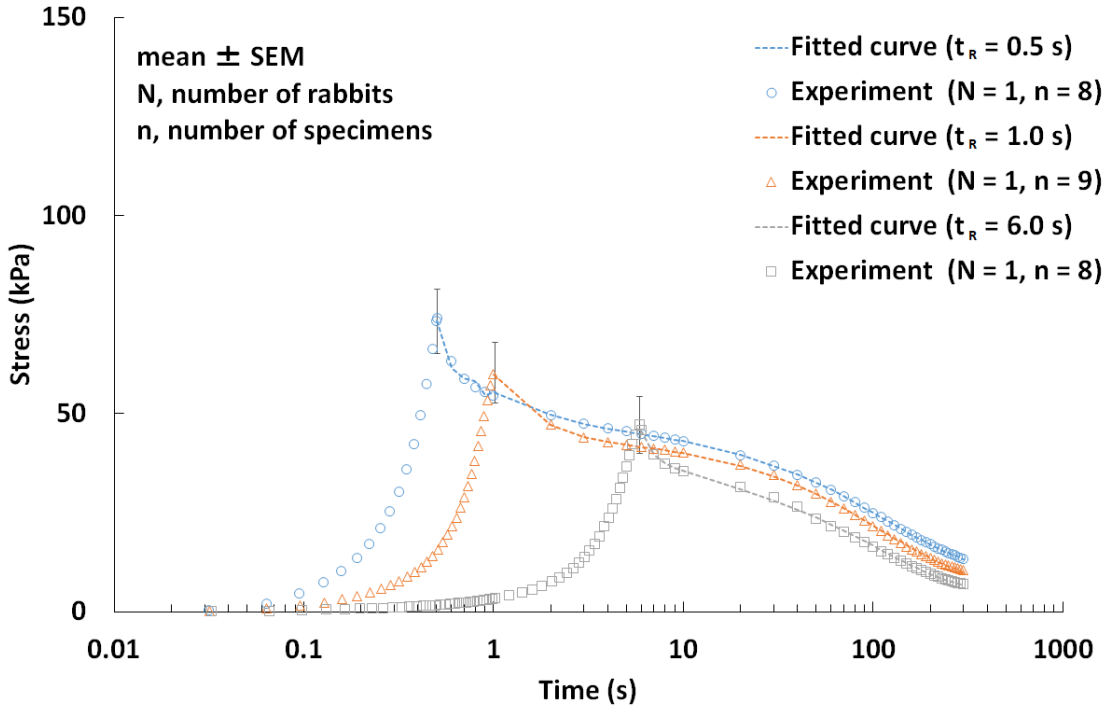

(a) Stress relaxation under a 6 mm stretch with the different rise times of t_R = 0.5, 1, and 6 s, which correspond to the rate of 12, 6, and 1 mm/s, respectively (N = 1).

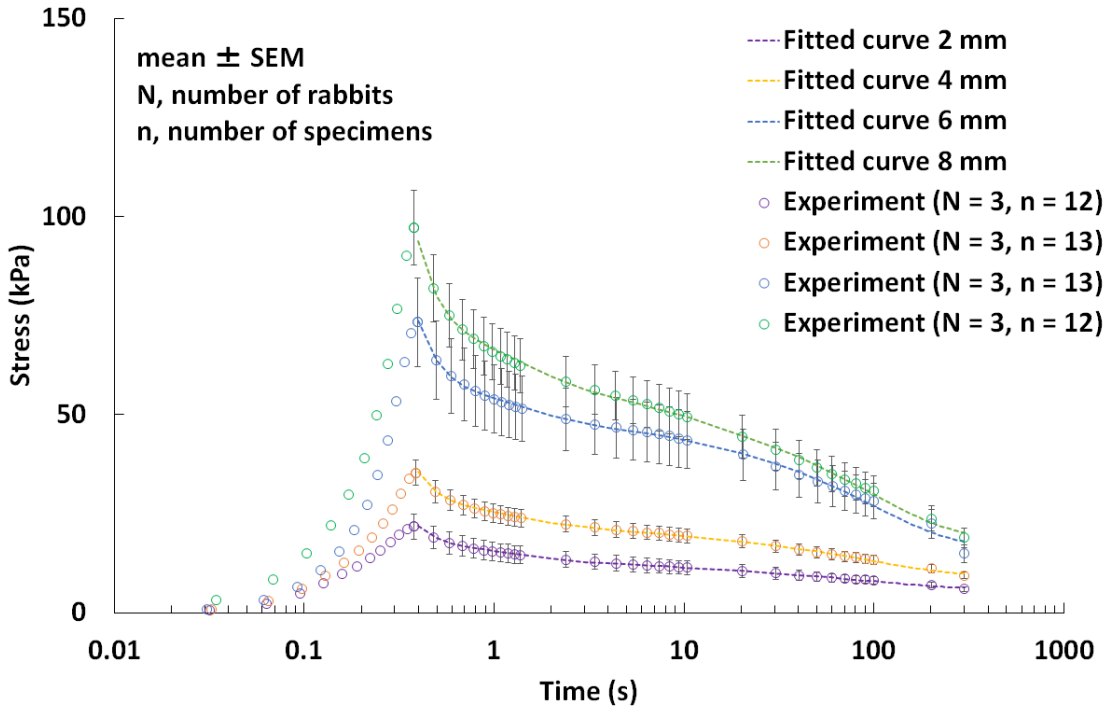

(b) Stress relaxation with four maximum stretches (2–8 mm) with a constant rise time of t_R = 0.4 s (N = 3).

Fig. 4: Stress relaxation over time (mean ± SEM) based on a preliminary study and an additional series of ramp-hold mechanical tests (present main study). Stress relaxation response of a muscle fiber bundle evidently depended on both the rate and the magnitude of a given stretch.

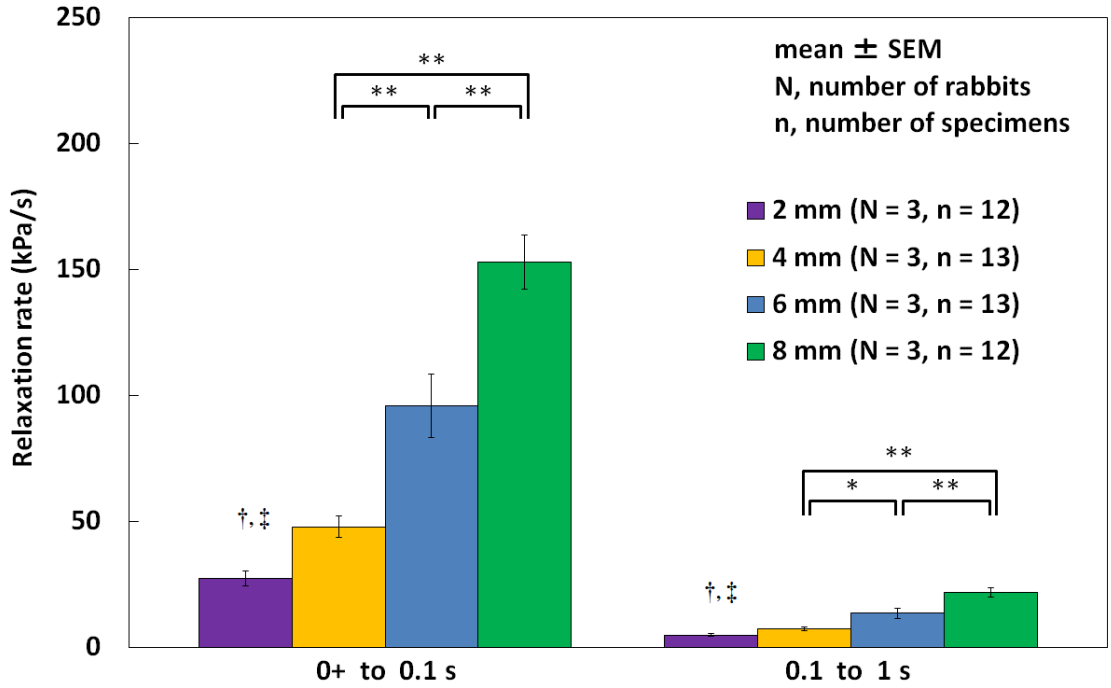

(a) Stress relaxation rates during the short intervals of 0_{+}–0.1 and 0.1–1 s (*$P < 0.05$ and **$P < 0.01$).

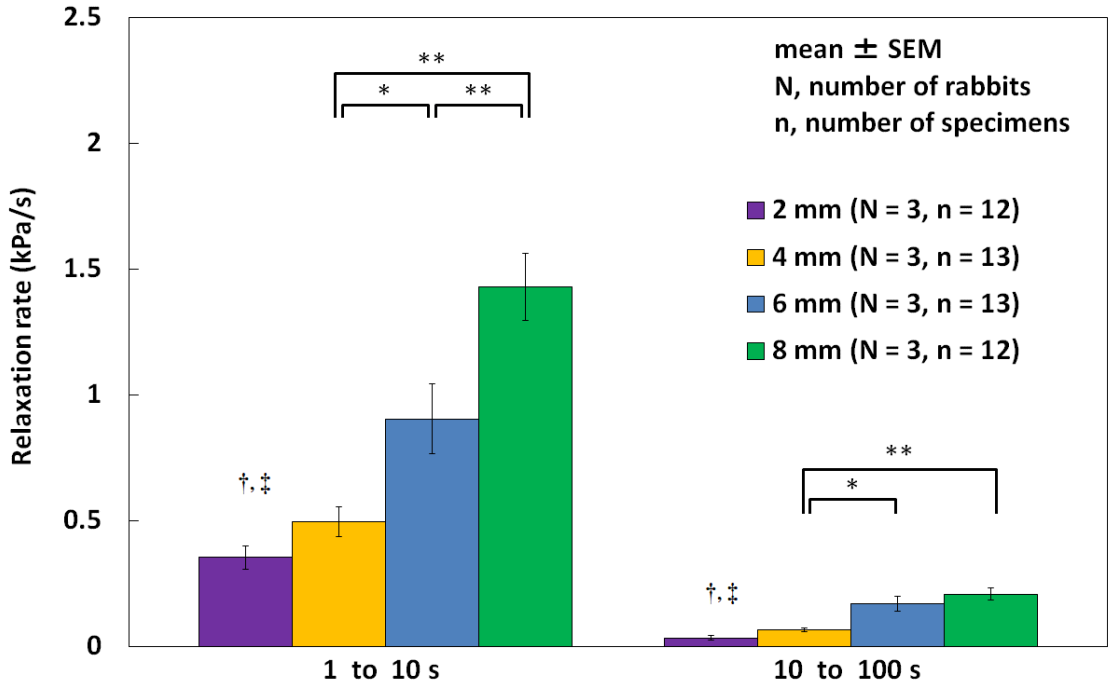

(b) Stress relaxation rates during the long intervals of 1–10 and 10–100 s (*$P < 0.05$ and **$P < 0.01$).

Fig. 5: Comparison of the stress relaxation rates after a constant rise time (t_R = 0.4 s) for applied maximum stretch of 2–8 mm ($N = 3$); † and ‡ indicate $P < 0.01$ compared to 6 and 8 mm stretches. Most

of the stress relaxation occurred during the very early stage of the mechanical test.

3.3 *Curve fitting to the stress relaxation responses*

Ramp-hold mechanical responses with a maximum stretch of 6 mm and rise times, t_R = 0.5, 1, and 6 s, were predicted using a custom program coded in MATLAB and compared with the measured stress relaxation responses obtained from the preliminary study. In Fig. 4a, the open circles with error bars represent the mean ± SEM of the experimental data while the dashed lines show the approximate fitted functions. It should be noted that the magnitude of the instantaneous stress response decreased gradually as the applied loading rate decreased. The theoretical curves indicate that the time-dependent mechanical response can be accurately predicted for various rise times, i.e., the curve fitting employed here could effectively capture the behavior of the data over the entire experiment.

As a next step, the stress relaxation responses were similarly predicted for various maximum stretches in the range of 2–8 mm using an approach used for the various rise times in the range of 0.5–6 s (Fig. 4b). The results confirmed that theoretical curves were reasonably comparable with the experimental data, including that during the ramp phase (Fig. 6). Notably, the viscoelastic mechanical responses during the holding period were successfully reproduced within the range of test configurations, indicating that the proposed curve fitting method provides good predictions that are consistent with those obtained using the theoretical model, thus verifying the performance of the proposed approach.

3.4 *Predicted elastic response*

The material stiffness parameters, E_i (i = 1–5), and corresponding elastic responses, σ_0 (t = 0), are summarized in Table 1. Both of these properties were affected by the loading rate and the magnitude of the maximum stretch as evidenced by the behavior of the reduced relaxation modulus (Fig. 3) and the stress relaxation rate (Fig. 5). Based on the combination of identified coefficients E_i (i = 1–5), the maximum stress corresponding to an idealized step-like input can be computed theoretically by substituting t = 0 into Eq. 6. Further, the elastic stress–strain response can be predicted using a quadratic function with the least-squares method under the assumption that muscle fiber bundles fail at a 54% tensile strain (Tamura et al., 2016). As demonstrated in Fig. 7, the maximum stress reached approximately 400 kPa at failure, which is equivalent to the maximum isometric contraction stress of skeletal muscle as reported elsewhere (Myers et al., 1998; Spyrou and Aravas, 2011; Davidovits, 2012).

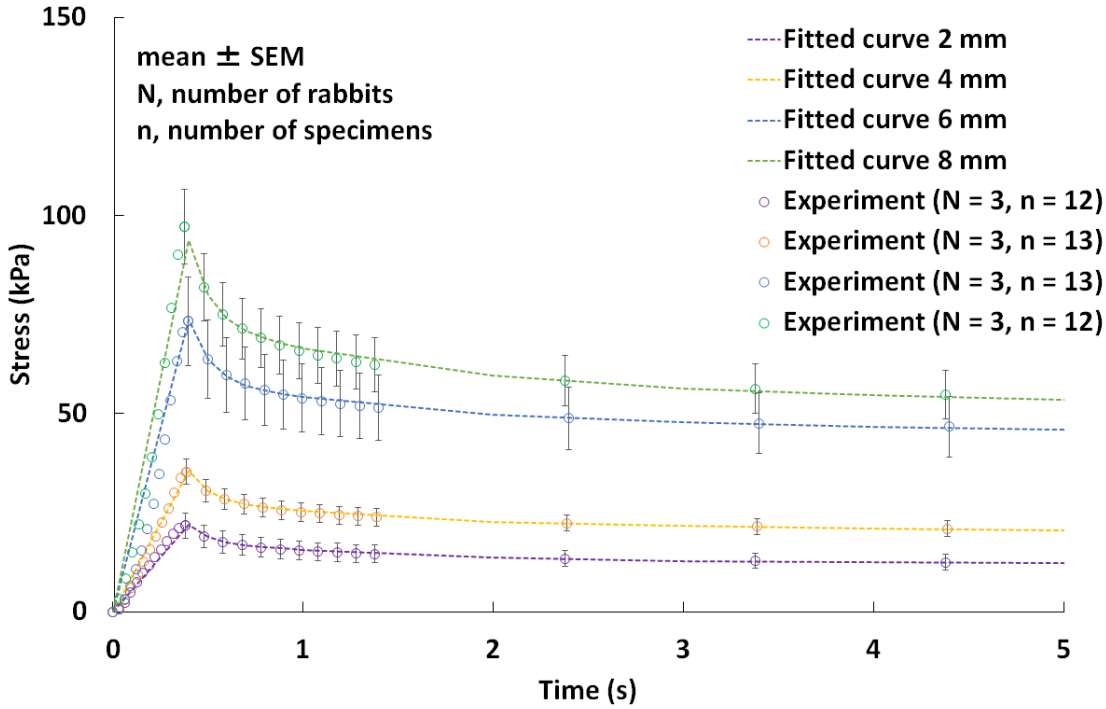

Fig. 6: Comparison of the stress relaxation (mean ± SEM) over time in the early loading phase (t = 0–5 s) obtained with a constant rise time of t_R = 0.4 s and four different maximum stretches 2–8 mm (N = 3). Theoretical curves fitted well with the recorded experimental responses, including the ramp-hold phase.

Table 1: Identified stiffness coefficients E_i (i = 1–5) and estimated elastic response, σ_0, with four different maximum stretches (N = 3).

Stretch%	E_1 (kPa)	E_2 (kPa)	E_3 (kPa)	E_4 (kPa)	E_5 (kPa)	σ_0 (kPa)
8% (2 mm)	284.1	67.1	34.8	34.8	97.9	41.5
16% (4 mm)	250.9	43.6	26.0	39.0	76.0	69.7
24% (6 mm)	338.9	47.5	26.7	90.7	89.5	142.4
32% (8 mm)	336.9	56.7	37.7	71.4	75.8	185.2

The instantaneous stress, σ_0, was obtained by substituting t = 0 into Eq. 6 and was specific to each of the applied stretches (2, 4, 6, and 8 mm). E_i (i = 1–5) and τ_i (τ_1 = 0.1, τ_2 = 1, τ_3 = 10, τ_4 = 100, and τ_5 = 1000 s) correspond to each other.

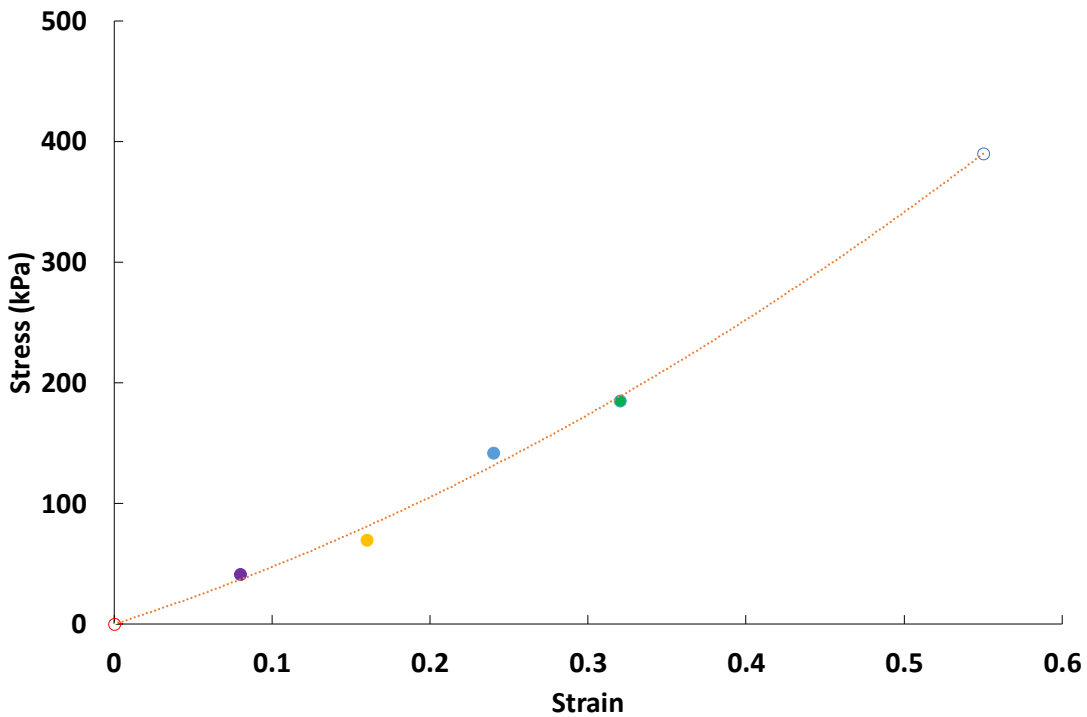

Fig. 7: Passive elastic response typical of a traumatic loading event as predicted by curve fitting; the solid circles were obtained based on a series of stress relaxation tests with a constant rise time, t_R = 0.4 s, and four maximum stretches (2, 4, 6, and 8 mm) as summarized in Table 1. Peak stress would be on the order of 300–500 kPa at the maximum stretch, i.e., 54% engineering strain.

4. Discussion

To precisely model highly dynamic or ballistic human movements using computational models, it is important to elucidate the mechanical responses of a skeletal muscle under high-rate loading regimes. Technically, however, to ramp the loading so rapidly is challenging and is likely to result in an overshoot in the applied displacement and the introduction of inevitable oscillations and contamination of the recorded data. Therefore, in practice, the initial input strain is usually more like a moderate ramp loading with a finite rise time that varies in terms of the strain rate, depending on the context of the study. Wheatley et al. (2016) conducted a series of stress relaxation tests using a tibialis anterior muscle tissue extracted from New Zealand white rabbits. Specimens were subjected to five steps ramp-hold cycles followed by a 300 s relaxation period. Their data typically showed 5–10 kPa for peak stress and 2–3 kPa for equilibrium stress at 10% strain, which is much smaller than our data because the tissues were elongated at the rate of 3.8 mm/s (~0.1 s^{-1}) in their mechanical test. On the other hand, the relaxation ratio, σ_{300}/σ_{0+} (the stress measured at 300 s divided by the peak stress obtained at t_R = ~1 s), showed no

dependence on the applied strain and had a mean value of 0.211. This is comparable with the relaxation ratio, σ_{300}/σ_{0+} = 0.250, obtained here (Fig. 3b). Abraham et al. (2013) also assessed the viscoelastic properties of muscle tissue isolated from New Zealand white rabbit hind limbs upon extension and reported that approximately 40% of the stress relaxation occurs during the first 100 s of the ramp-hold phase. Since they used whole and sectioned muscles as test specimens, the ramp loading was applied with a rise time of 10 s. On the contrary, it takes about 20 s to reach 40% stress relaxation against the ramp loading in our experiments (Fig. 3b), suggesting that a considerable amount of stress relaxation may have occurred during the very early stage following the applied loading. This is also in contrast to the results of a study by Tian et al. (2010, 2011) on the passive mechanical properties of human gastrocnemius muscle–tendon units *in vivo*. By applying the QLV model to the experimental data, Tian et al. concluded that the loading rate does not have a significant effect on the muscle–tendon unit over the range of velocities tested. However, as the initial displacement was applied manually in their experimental setup, a rise time of t_R = 3.4 ± 1.1 s (mean ± SD) was required before reaching the peak load. Moreover, the data was analyzed after $3t_R$ = 10.2 s, meaning that the effective rise time was on the order of 10 s. Thus, the intrinsic viscous effects might have been overshadowed because the initial stress relaxation occurred during the early stage after applying the manual displacement. Indeed, the authors noted that the data reported in that study should not be interpreted as indicating that viscous effects are not important in muscle mechanics because their samples were muscle–tendon units; a broad spectrum of relaxation processes occurring within muscle tissue are associated with its hierarchical structure, which comprises micro to macro components of different lengths and structural scales, e.g., a sarcomere, myofibril, fiber, fascicle (fiber bundle), tissue, whole muscle, and muscle–tendon unit (Bilston and Tan, 2014). Thus, our findings suggest that the viscous effect is dominant in the scale of muscle fiber bundles.

In our prior work (Tamura et al., 2016), we have shown that the ultimate tensile strain of muscle fiber bundles was almost constant at approximately 54% regardless of the magnitude of the externally applied loading rate. On the other hand, the tensile strength differed with the rate and was on the order of 100–200 kPa. Meyers et al. (1998) investigated the effect of the strain rate on the tibialis anterior muscles of New Zealand white rabbits *in vivo*. Their results indicated that the stress–strain response of passive skeletal muscle is quite sensitive to the stretching velocity over a range of strain rates (1–25 s^{-1}). Moreover, the failure stress was in the range of 0.5–1.1 MPa, which was higher than the tensile strength that we reported previously. In the Meyers et al. study, the exposed almost intact muscle–tendon unit was used as the test specimen *in vivo*; thus, it was protected by stiff membranous materials such as the

epimysium and aponeurosis. However, the muscle fiber bundles that were used in the experiments presented here were isolated from tissue samples so they contained relatively less stiff membranous materials and included endomysium and perimysium but did not contain epimysium and aponeurosis. Therefore, the difference in the reported mechanical failure stresses may be partly attributable to the additional strength provided by the extracellular matrix remaining in the test samples in the Meyers et al. study. The difference may also be ascribed to the rate dependence of the muscle fiber bundle of itself. If it is assumed that the failure strain is constantly at 54%, the tensile strength in a considerably high-rate loading regime would be on the order of 300–500 kPa (according to Fig. 7). Since this is equivalent to the maximum isometric contraction stress at an optimum length that was previously reported by Meyers et al. (1998), 440 ± 150 kPa (mean ± SD), it appears that the predicted failure stress fell within the range of reasonable values in terms of passive mechanical properties. In fact, our previous study (Tamura et al., 2016) showed that the axial strain is distributed nonuniformly, even in a relaxed state when subjected to uniaxial stretching. This suggests that the nonuniformity of the strain distribution will be increased when the specimen is activated (i.e., contracted). Since the isometric axial load is essentially constant and balanced between both ends along the fiber direction regardless of the inhomogeneous strain distribution, the lack of an active contraction force must be compensated with a passive resistance force due to the additional elongation that is generated locally. At a sarcomere level, this nonuniformity-related phenomenon can be explained by the hypotheses of sarcomere popping and residual force enhancement, i.e., partially weak sarcomere or loose overlap between the thin and thick myofilaments stemming from focal overstretching at the intracellular level can be mechanically compensated for at the expense of the lengthening of the weakened sarcomeres of themselves (Givli, 2014). Since it can be expected that the macroscopic behavior of skeletal muscle is dictated by its microscopic properties, the predicted tensile strength should be on the same order as the maximum isometric contraction stress. Of another note, according to Meyer et al. (2011), a single muscle fiber passively shows instantaneous stresses of 70 kPa and 140 kPa when stretched at 30% and 50%, respectively, at a rate of 20 s^{-1}. Based on the theoretical elastic response (Fig. 7), it can be estimated that a muscle fiber bundle would show instantaneous stresses of 170 kPa and 340 kPa at 30% and 50% strains, respectively. Thus, fibers would bear approximately 40% of the applied load and the intramuscular connective tissues would bear the rest of it, i.e., ~60%. However, a further study will be required to precisely account for the contribution from each component independently, and it is difficult to conclude at this stage.

There are couple of limitations to be addressed in this study. First, as shown in Figure 4, we observed

relatively significant deviations from the mean value in measured test data. In the current work, we minimized the potential difference among specimens by limiting the number of rabbits (N = 3) and the effect of rigor mortis by keeping a specimen's natural length in the relaxing solution. We also well preconditioned specimens prior to conducting stress relaxation tests. Nevertheless, specimens might be degraded during the whole process of the mechanical test, because approximately 30 h were required to complete all the experiments after animal sacrifice. Another limitation is that our model is one-dimensional, while the skeletal muscle is inherently three-dimensional with a finite deformation as described in previous studies (Ferreira et al., 2017; Pouca et al., 2018). Since the material anisotropy and visco-hyperelasticity are also a critical factor for representing a muscle tissue *in vivo*, we need to take into account of it along with the effect of active contraction. The theoretical model proposed here, however, can be applied to a hyperelastic material, and we can easily implement a viscous effect in the constitutive law. In the future, stress relaxation tests should be conducted using greater stretch magnitudes around 10–12 mm to encompass the entire elongation process up to the material failure. Nevertheless, extended stretches greater than 10 mm could cause micro-cracks or other damage in the fiber bundle specimen. Thus, to ensure the repeatability of the mechanical testing, the elastic tensile behavior in response to an idealized step-like input was obtained by extrapolation. During traumatic events, skeletal muscle may experience high strains over a short period. To represent impact-induced injury, replicating a ballistic loading condition is desirable; however, application of such loading condition would contaminate the test results. Due to the lack of experimental data at strain rates that may cause injury ($\dot{\varepsilon} > 10\ \mathrm{s}^{-1}$, which is typical of a traumatic impact), the overall *in vivo* mechanics of traumatic injuries is still unclear. Therefore, this is the first study, based on relatively moderate loading conditions, to present critical information about the elastic tensile behavior of muscle fiber bundles and the stress–strain relationship typical of traumatic impact events.

5. Conclusions

We conducted a series of stress relaxation tests using freshly isolated muscle fiber bundles and demonstrated the applicability of the proposed fitting procedure to correct for the finite-ramp effect on the experimental stress relaxation. The experimental results revealed that muscle fiber bundles reach about 400 kPa at the maximum stretch and that a considerable amount of stress relaxation may occur during the initial ramp period immediately after the rise time. Hence, to precisely predict the behavior of the human body under ballistic events using a computational model, it is important to take into consideration the

effects of the initial stress relaxation, which contribute to the muscle's role as an intrinsic damper or stabilizer in the human musculoskeletal system.

Acknowledgments

Funding: This study was financially supported in part by AMED-CREST [JP18gm081005h0403]. There are no conflicts of interest to declare. The authors deeply thank Mr. Sadayuki Hayashi, Toyota Central R&D Labs., Inc., for his technical advice and sincere comments given on this study.

References

[1] Abraham AC, Kaufman KR, and Haut Donahue TL "Phenomenological consequences of sectioning and bathing on passive muscle mechanics of the New Zealand white rabbit tibialis anterior," Journal of the Mechanical Behavior of Biomedical Materials **17** (2013) pp. 290-295. DOI: 10.1016/j.jmbbm.2012.10.003

[2] Bilston LE and Tan K "Measurement of passive skeletal muscle mechanical properties *in vivo*: Recent progress, clinical applications, and remaining challenges," Annals of Biomedical Engineering **43** (2014) pp. 261-273. DOI: 10.1007/s10439-014-1186-2

[3] Davidovits P "Physics in Biology and Medicine, 4th ed.," Academic Press (2012) Burlington, MA (USA).

[4] Ferreira JPS, Parente MPL, Jabareen M, and Natal Jorge RM "A general framework for the numerical implementation of anisotropic hyperelastic material models including non-local damage," Biomechanics and Modeling in Mechanobiology **16** (2017) pp. 1119–1140. DOI: 10.1007/s10237-017-0875-9

[5] Fung YC "Elasticity of soft tissues in simple elongation," American Journal of Physiology **213** (1967) pp. 1532-1544. DOI: 10.1152/ajplegacy.1967.213.6.1532

[6] Fung YC "Biomechanics: Mechanical Properties of Living Tissues, 2nd ed.," Springer-Verlag (1993) New York, NY (USA). DOI: 10.1007/978-1-4757-2257-4

[7] Funk JR, Hall GW, Crandall JR, and Pilkey WD "Linear and quasi-linear viscoelastic characterization of ankle ligaments," Journal of Biomechanical Engineering **122** (2000) pp. 15-22. DOI:10.1115/1.429623

[8] Givli S "Contraction induced muscle injury: Towards personalized training and recovery program," Annals of Biomedical Engineering **43** (2014) pp. 388-403. DOI: 10.1007/s10439-014-1173-7

[9] Lai AKM, Arnold AS, Biewener AA, Dick TJM, and Wakeling JM "Does a two-element muscle model offer advantages when estimating ankle planar flexor forces during human cycling?" Journal of Biomechanics **68** (2018) pp. 6-13. DOI: 10.1016/j.jbiomech.2017.12.018

[10] LaStayo PC, Woolf JM, Lewek MD, Snyder-Mackler L, Reich T, and Lindstedt SL "Eccentric muscle contractions: Their contribution to injury, prevention, rehabilitation, and sport," Journal of Orthopaedic & Sports Physical Therapy **33** (2003) pp. 557-571. DOI: 10.2519/jospt.2003.33.10.557

[11] Lieber RL "Muscle fiber length and moment arm coordination during dorsi- and plantarflexion in the mouse hindlimb," Acta Anatomica **159** (1997) pp. 84-89. DOI: 10.1159/000147970

[12] Meyer GA, McCulloch AD, and Lieber RL "A nonlinear model of passive muscle viscosity," Journal of Biomechanical Engineering **133** (2011) pp. 091007-1-9. DOI: 10.1115/1.4004993

[13] Meyers BS, McElhaney JH, and Doherty BJ "The viscoelastic responses of the human cervical spine in torsion: Experimental limitations of quasi-linear theory, and a method for reducing these effects," Journal of Biomechanical Engineering **24** (1991) pp. 811-817. DOI: 10.1016/0021-9290(91)90306-8

[14] Meyers BS, Wooley CT, Slotter TL, Garrett WE, and Best TM "The influence of strain rate on the passive and stimulated engineering stress–large strain behavior of the rabbit tibialis anterior muscle," Journal of Biomechanical Engineering **120** (1998) pp. 126-132. DOI: 10.1115/1.2834292

[15] Quapp KM and Weiss JA "Material characterization of human medial collateral ligament," Journal of Biomechanical Engineering **120** (1998) pp. 757-763. DOI: 10.1115/1.2834890

[16] Spyrou LA and Aravas N "Muscle and tendon tissues: Constitutive modeling and computational issues," Journal of Biomechanical Engineering **78** (2011) pp. 041015-1-10. DOI: 10.1115/1.4003741

[17] Tamura A, Omori K, Miki K, Lee JB, Yang KH, and King AI "Mechanical characterization of porcine abdominal organs," Stapp Car Crash Journal **46** (2002) pp. 50-70.

[18] Tamura A, Hayashi S, Watanabe I, Nagayama K, and Matsumoto T "Mechanical characterization of brain tissue in high-rate compression," Journal of Biomechanical Science and Engineering **2** (2007) pp. 115-126. DOI: 10.1299/jbse.2.115

[19] Tamura A, Hayashi S, Nagayama K, and Matsumoto T "Mechanical characterization of brain tissue in high-rate extension," Journal of Biomechanical Science and Engineering **3** (2008) pp. 263-274. DOI: 10.1299/jbse.3.263

[20] Tamura A, Hayashi S, and Matsumoto T "Effect of loading rate on viscoelastic properties and local mechanical heterogeneity of freshly isolated muscle fiber bundles subjected to uniaxial stretching,"

Journal of Mechanics in Medicine and Biology **16** (2016) pp. 1650086.
DOI: 10.1142/S021951941650086X

[21] Tamura A, Hongu J, Yamamoto T, and Koide T "Dynamic tensile behavior of fiber bundles freshly isolated from nerve roots," In: Proceedings of ASME 2017 International Mechanical Engineering Congress and Exposition (2017) Paper No. IMECE2017-70796, Tampa, FL (USA).
DOI: 10.1115/IMECE2017-70796

[22] Tian M, Hoang PD, Gandevia SC, Bilston LE, and Herbert RD "Stress relaxation of human ankles is only minimally affected by knee and ankle angle," Journal of Biomechanics **43** (2010) pp. 990-993.
DOI: 10.1016/j.jbiomech.2009.11.017

[23] Tian M, Hoang PD, Gandevia SC, Herbert RD, and Bilston LE "Viscous elements have little impact on measured passive length–tension properties of human gastrocnemius muscle–tendon units *in vivo*," Journal of Biomechanics **44** (2011) pp. 1334-1339. DOI: 10.1016/j.jbiomech.2011.01.005

[24] Troyer KL, Estep DJ, and Puttlitz CM "Viscoelastic effects during loading play an integral role in soft tissue mechanics," Acta Biomaterialia **8** (2012) pp. 234-243. DOI: 10.1016/j.actbio.2011.07.035

[25] Vila Pouca MCP, Ferreira JPS, Oliveira DA, Parente MPL, Mascarenhas T, and Natal Jorge RM "On the effect of labour durations using an anisotropic visco-hyperelastic-damage approach to simulate vaginal deliveries," Journal of the Mechanical Behavior of Biomedical Materials **88** (2018) pp. 120–126. DOI: 10.1016/j.jmbbm.2018.08.011

[26] Wheatley BB, Marrow DA, Odegard GM, Kaufman KR, and Haut Donahue TL "Skeletal muscle tensile strain dependence: Hyperviscoelastic nonlinearity," Journal of the Mechanical Behavior of Biomedical Materials **53** (2016) pp. 445-454. DOI: 10.1016/j.jmbbm.2015.08.041